iScience

CellPress
OPEN ACCESS

Article

PhotoGal4: A Versatile Light-Dependent Switch for Spatiotemporal Control of Gene Expression in *Drosophila* Explants

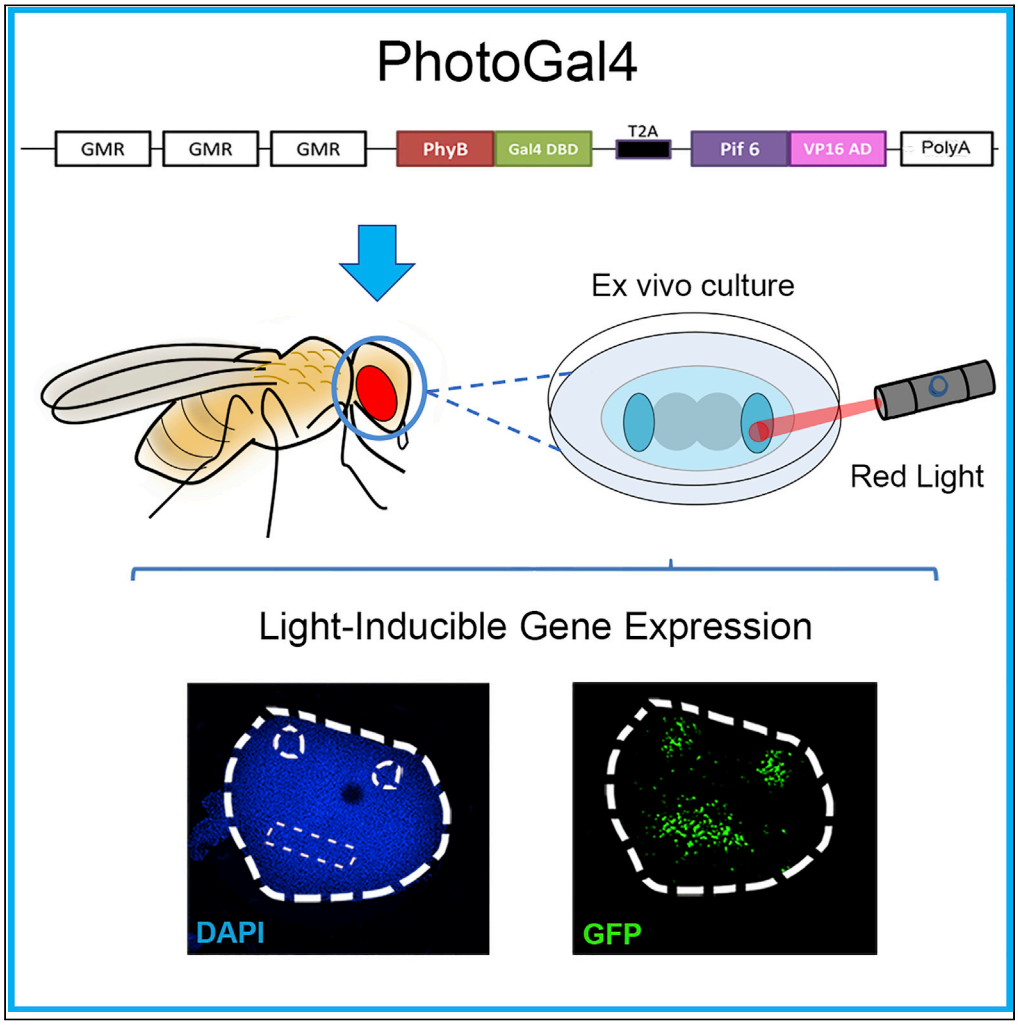

Lorena de Mena, Diego E. Rincon-Limas

lorena.demenaalvarez@neurology.ufl.edu (L.d.M.)
diego.rincon@neurology.ufl.edu (D.E.R.-L.)

HIGHLIGHTS

PhotoGal4 activates gene expression in response to red light in *Drosophila* explants

Exposure to far-red light allows for PhotoGal4 deactivation

PhotoGal4 can activate gene expression in subgroups of cells within a single tissue

de Mena & Rincon-Limas, iScience *23*, 101308
July 24, 2020
https://doi.org/10.1016/j.isci.2020.101308

iScience

CellPress
OPEN ACCESS

Article

PhotoGal4: A Versatile Light-Dependent Switch for Spatiotemporal Control of Gene Expression in *Drosophila* Explants

Lorena de Mena[1,*] and Diego E. Rincon-Limas[1,2,3,4,*]

SUMMARY

We present here PhotoGal4, a phytochrome B-based optogenetic switch for fine-tuned spatiotemporal control of gene expression in *Drosophila* explants. This switch integrates the light-dependent interaction between phytochrome B and PIF6 from plants with regulatory elements from the yeast Gal4/UAS system. We found that PhotoGal4 efficiently activates and deactivates gene expression upon red- or far-red-light irradiation, respectively. In addition, this optogenetic tool reacts to different illumination conditions, allowing for fine modulation of the light-dependent response. Importantly, by simply focusing a laser beam, PhotoGal4 induces intricate patterns of expression in a customized manner. For instance, we successfully sketched personalized patterns of GFP fluorescence such as emoji-like shapes or letterform logos in *Drosophila* explants, which illustrates the exquisite precision and versatility of this tool. Hence, we anticipate that PhotoGal4 will expand the powerful *Drosophila* toolbox and will provide a new avenue to investigate intricate and complex problems in biomedical research.

INTRODUCTION

As a powerful genetic model organism, *Drosophila melanogaster* continues to be a source of innovation in the development of gene expression systems, from the more traditional UAS/Gal4 approach to the more complex heat shock-, hormone- and chemical-related systems (Fischer et al., 1988; Osterwalder et al., 2001; Sun et al., 2007; Tanguay, 1988). Despite their functionality, these classical tools still have few caveats that impinge accurate spatiotemporal control of transgene expression. For example, with heat shock-dependent systems, full activation of transcription occurs only at high temperatures, which may trigger unwanted cellular stress. On the other hand, hormonal- and chemical-dependent promoters lack precise temporal transcriptional activation or deactivation and can be accompanied by complex pharmacokinetics and pleiotropic effects (Landis et al., 2015). Therefore a rapid and reversible inducible system that could offer fine spatiotemporal resolution without toxicity is urgently needed. In this regard, optogenetic approaches seem to check all the boxes. Optogenetics exploits photo-sensing proteins that change conformation in the presence of light to manipulate critical physiological processes in plants, fungi, and cyanobacteria. As these photo-sensing molecules use light as the activating force, inducible systems based on this principle are fast, accurate, and can be quickly reversed by simply removing the stimulus (de Mena et al., 2018; Pathak et al., 2013, 2014).

Among the vast optogenetic repertoire, phytochrome B (PhyB)-based tools have special interest owing to their high stability and unique light-dependent reversibility. In this case, a two-hybrid-like system capitalizes on the light-dependent heterodimerization between the photoreceptor PhyB from *Arabidopsis thaliana* and its interacting partner Pif6 (Hughes et al., 2012; Shimizu-Sato et al., 2002). Briefly, in the absence of light, PhyB exists in a red-absorbing form, known as Pr, in association with the endogenous chromophore phycocyanobilin (PCB) (Levskaya et al., 2009; Muller et al., 2013a). Then, upon red light irradiation (~630 nm), the Pr inactive form undergoes a conformational change switching into the active form (Pfr), which interacts with its cofactor Pif6 to exert a variety of functions (Auldridge and Forest, 2011; Davis et al., 1999). Conversely, when illuminated with far-red light (>730 nm), PhyB reverts to the inactive Pr form and dissociates from Pif6. Thus, based on the original design of Shimizu-Sato and co-workers (Shimizu-Sato et al., 2002), we combined the PhyB photosensory N-terminal domain with the Gal4-DNA

[1]Department of Neurology, McKnight Brain Institute, and Norman Fixel Institute for Neurological Diseases, University of Florida, Gainesville, FL 32611, USA

[2]Department of Neuroscience, Center for Translational Research in Neurodegenerative Disease, University of Florida, Gainesville, FL 32611, USA

[3]Genetics Institute, University of Florida, Gainesville, FL 32611, USA

[4]Lead Contact

*Correspondence: lorena.demenaalvarez@neurology.ufl.edu (L.d.M.), diego.rincon@neurology.ufl.edu (D.E.R.-L.)

https://doi.org/10.1016/j.isci.2020.101308

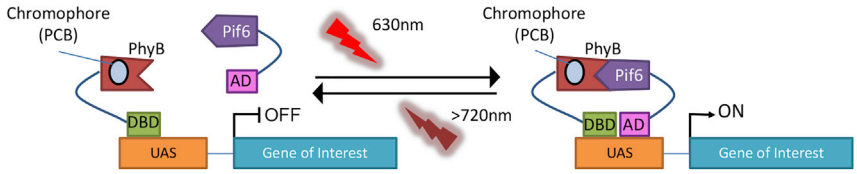

Figure 1. Schematic Representation of the PhotoGal4 Light-Dependent Gene Expression System

In the dark, phytochrome B (PhyB) remains in its inactive form. Upon incorporation of the chromophore PCB and red light (~630nm) stimulation, PhyB undergoes a conformational change, turning into the active form. Then, PhyB heterodimerizes with phytochrome-interacting factor 6 (Pif6) to bring together the Gal4 DNA binding domain (DBD) and VP16 activation domain (AD) at the UAS binding sequence, which triggers transcription of the gene of interest. Conversely, upon far-red (>730 nm) illumination, PhyB and Pif6 dissociate, halting transcription immediately.

binding domain (Gal4-DBD) and PIF6 with the VP16 activator domain (Pif6-VP16 AD) to engineer a bicistronic system (Figure 1). This resulted in a tunable light-dependent regulator of gene expression with rapid ON/OFF kinetics and reduced background.

Here, we introduce PhotoGal4 as a highly sensitive and flexible PhyB-based light-dependent system for spatiotemporal control of gene expression in fruit fly tissues. As a proof of concept, we used *Drosophila ex vivo* tissue cultures to show how gene expression can be successfully adjusted in a light- and chromophore-dependent manner at different stages of development in the eye. Importantly, we found that manipulation of light frequency and intensity allows for fine-tuned control over the expression levels of the target gene. Moreover, targeting illumination at confined areas within the eye disc triggered PhotoGal4-mediated transcription in selected subset of cells, resulting in personalized sub-patterns of gene expression. Therefore, we anticipate that PhotoGal4 will be a valuable resource to investigate complex biological, developmental, and pathological processes in *ex vivo* paradigms with remarkable resolution.

RESULTS

Engineering and Validation of PhotoGal4 in *Drosophila* Cultured Cells

Our PhyB-based inducible system, PhotoGal4, consists of a single bicistronic vector encoding for PhyB fused to the Gal4-DNA binding domain (PhyB-Gal4 DBD) and Pif6 fused to the VP16 transcriptional activator domain (Pif6-VP16 AD) (Figure 2A). In our design, we opted for a previously reported form of PhyB that contains N-PAS2-GAF-PHY motifs, but lacks PAS and histidine kinase-related domains (Beyer et al., 2015). This truncated PhyB (1–650 amino acid [aa]) was previously reported to have a more robust and consistent expression than its full-length counterpart (Buckley et al., 2016). We also chose a shorter form of Pif6 consisting only of its activated phytochrome binding domain. This truncated form of Pif6 (1–100 aa) can still associate with PhyB while maintaining its photo-reversible capabilities (Levskaya et al., 2009). Thus, the chimeric PhyB-Gal4 DBD and Pif6-VP16 AD sequences tagged, respectively, with HA and V5 were subcloned into an actin expression vector separated by the ribosomal skipping sequence T2A (Figure 2A), which allows expression of both proteins under a single promoter. Therefore, the resulting construct includes all the required components to trigger light-dependent activation of any UAS transgene. We first confirmed that both hybrid proteins (PhyB-Gal4DBD-HA and Pif6-VP16AD-V5) are produced in PhotoGal4-transfected S2R+ cells through western blot and immunohistochemistry (Figures 2B and 2C). Next, to test the light-dependent activity of PhotoGal4, we co-transfected *Drosophila* S2R+ cells with the PhotoGal4 vector and a reporter plasmid carrying UAS-Luciferase. Due to the absence of the chromophore PCB in animal cells, this compound was provided exogenously to allow PhyB-Pif6 interactions (Shimizu-Sato et al., 2002). Thus, 20 h after transient transfection, we supplemented the S2R+ cell culture medium with 10 μM PCB. As expected, transfected cells supplemented with PCB and irradiated with pulses of red light (10 s ON/10 s OFF, 0.75 mW cm^{-2}) for an extra 24 h showed an ~20-fold increase in Luciferase expression ($p > 0.01$) compared with cells kept in total darkness or lacking PCB. Moreover, transfected cells cultured in dark conditions or without PCB showed similar Luciferase levels to cells transfected with the Luciferase vector alone (Figure 2D). This result suggests that PhotoGal4 activity relies entirely on light and PCB for transcriptional activation.

Characterization of PhotoGal4 Expression in *Drosophila Ex Vivo* Cultures

Drosophila ex vivo cultures are powerful experimental paradigms that facilitate long-term imaging and real-time analysis of a wide variety of processes such as cell migration, cell competition, circadian

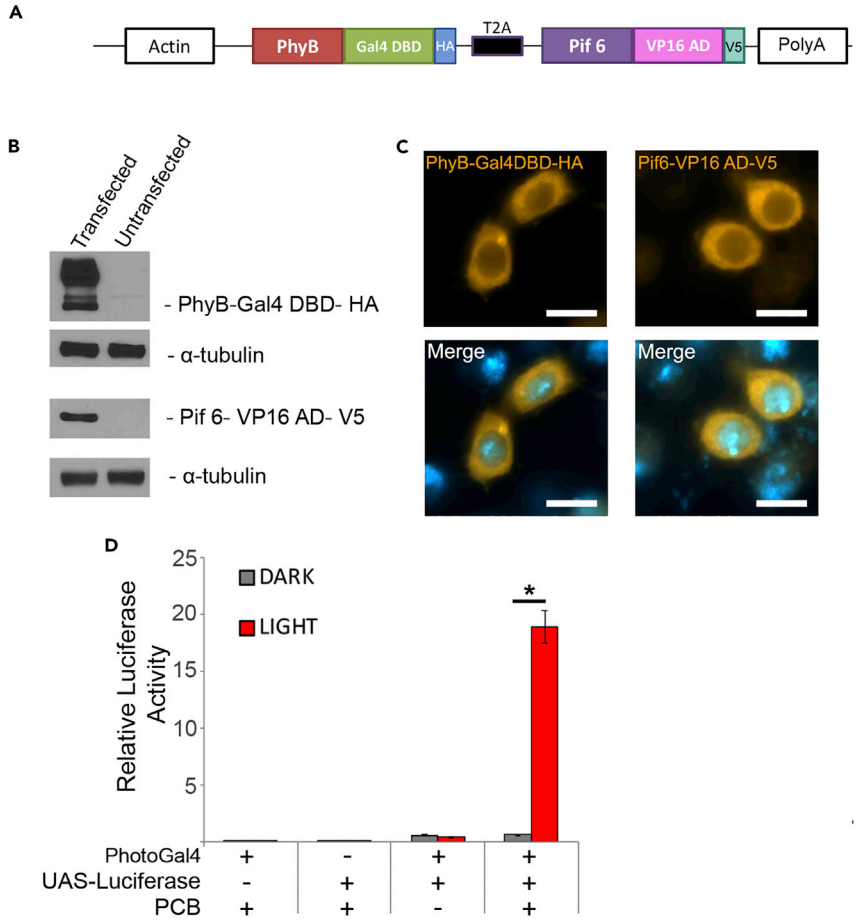

Figure 2. Light-Dependent Activation of PhotoGal4 in S2R+ Cells

(A) Schematic diagram of the Actin-PhotoGal4 construct. The Actin promoter regulates PhotoGal4, which consists of PhyB-650 amino acid fused to Gal4 DBD and the hemagglutinin (HA) tag on one side and the transcriptional activation domain of VP16 fused to Pif6 and the V5 tag on the other side, separated by the T2A sequence.

(B) Western blot analysis of PhotoGal4 components upon transient transfection in S2R+ cells. Untransfected cells were used as a negative control, and α-tubulin was used as internal control.

(C) Immunodetection of PhyB-Gal4DBD-HA and Pif6-VP16AD-V5 in S2R+ cells with anti-HA (left panel, Alexa 564) and anti-V5 (right panel, Alexa 564) antibodies. Scale bar, 10 μm.

(D) Luciferase activity levels in cells transfected only with PhotoGal4, UAS-Luciferase, or both. The plasmid pAC-renilla was used as control for normalization. After transfection, cells were kept in the dark or illuminated with red light pulses (630 nm; 10 s ON 10 s OFF) and cultured in media supplemented with PCB or DMSO for 24 h. Average levels of triplicates for luciferase activity are shown. *$p < 0.01$ by two-tailed Student's t test. All data are represented as mean ± S.D.

oscillations, developmental remodeling, and wound healing to name a few (Mezan et al., 2016; Prithviraj et al., 2012; Stramer and Wood, 2009; Tsao et al., 2016, 2017). Thus, we reasoned that implementation of PhotoGal4 in *Drosophila ex vivo* cultures would provide a new opportunity to address key questions in complex multicellular organs and tissues. Given the relatively flat structure of the eye imaginal disc in *Drosophila*, we tested our prototype system in this experimental context. As a first step, we created transgenic flies bearing the PhotoGal4 cassette under the control of three copies of the eye-specific GMR promoter (Figure S1A). Then, we proved that both PhyB-Gal4DBD and Pif6-VP16 AD were successfully expressed in these flies through western blots (Figure S1B). Moreover, protein distribution was restricted to cells posterior to the morphogenetic furrow, consistent with the expression domain of the GMR promoter in the developing larval eye disc (Hay et al., 1994) (Figure S1C). Of note, none of the seven GMR-PhotoGal4 lines (Figure S1D) created display any apparent changes in morphology, structure, and organization of the adult eye even in homozygosis (Figure S1E), suggesting that PhotoGal4 is innocuous in flies.

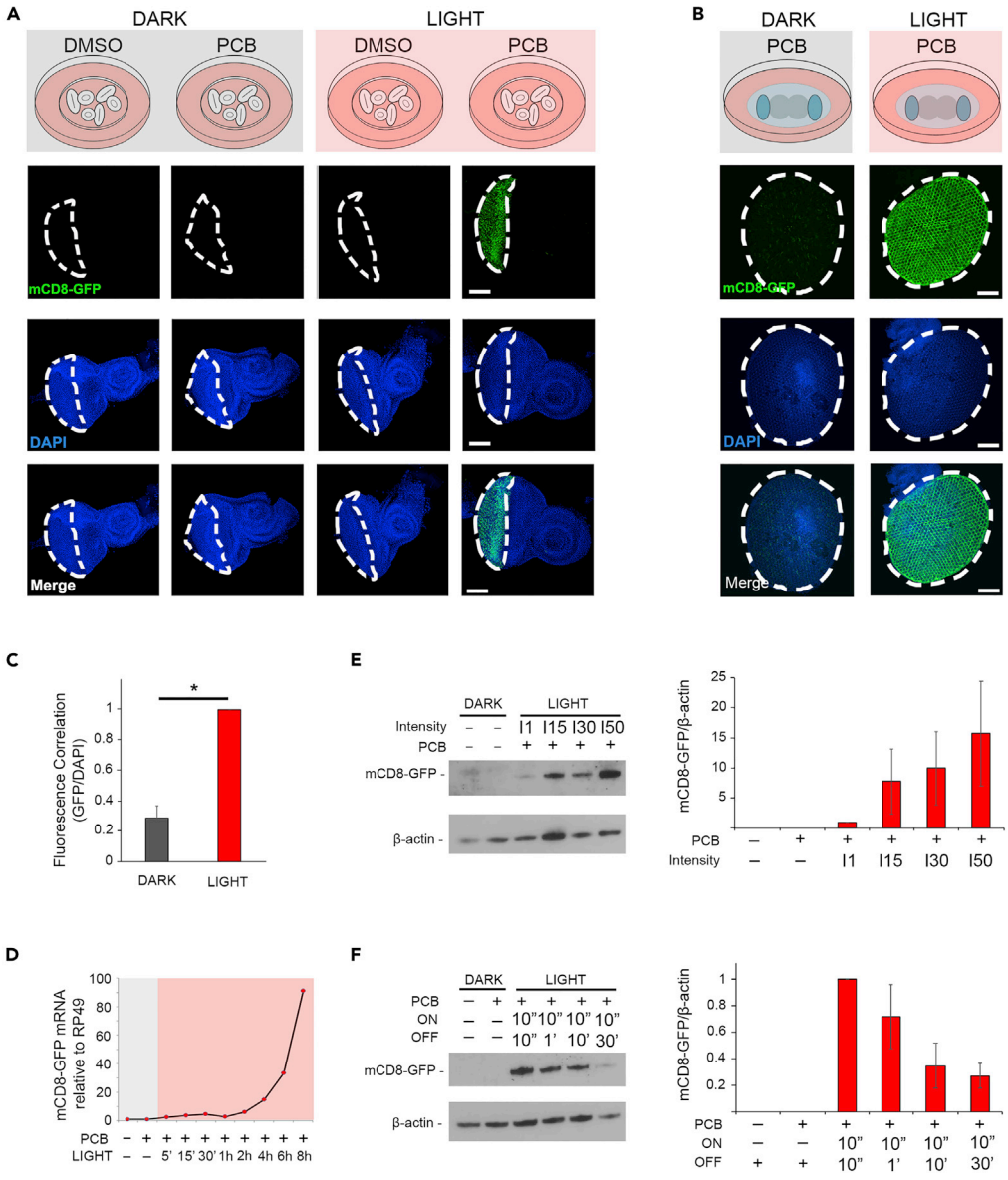

Figure 3. PhotoGal4 Activates Gene Expression in the Developing Eye of *Drosophila* in a Light-Dependent Manner

(A and B) Imaginal discs (A) or prepupal retinas (B) from flies expressing PhotoGal4 and UAS-mCD8-GFP constructs were dissected and grown in *ex vivo* culture media supplemented with 100 μM PCB or DMSO, either in the dark or under constant pulses of red light for 15 h (10 s ON, 10 s OFF) (n = 6 for each condition). Each image is the result of a projection of a z stack capture. White dotted lines mark the area where the GMR promoter drives PhotoGal4 expression. Scale bar, 100 μm.

(C) Relative fluorescence correlation for GFP protein levels of prepupal retinas cultured in dark or illuminated with red light in the presence of PCB. *$p < 0.01$ by two-tailed Student's t test. All data are represented as mean ± S.D.

(D) Light response curve of CD8-GFP transcription at different periods of illumination. Groups of 10 imaginal eye discs were cultured for a total of 8 h and exposed to continuous pulses of red light (~630nm 10s ON, 10s OFF) for the indicated amount of time (5′, 15′, 30′, 1 h, 2 h, 4 h, 6 h or 8 h). Controls were kept in dark for the entire duration of the experiment. mRNA levels were quantified by qPCR. Fold changes in GFP mRNA relative to the internal control RP49 are shown.

(E) Expression and quantification of CD8-GFP in response to increasing light intensities (I1, I15, I30, and I50). Groups of 10 eye discs were illuminated for 8 h with continuous light pulses (~630 nm 10 s ON, 50 s OFF) at the indicated intensities. Control samples were kept in dark during the whole experiment, and β-actin was used as internal control for normalization. All data are represented as mean ± S.D.

Figure 3. *Continued*

(F) Expression and quantification of CD8-GFP in response to the frequency of light pulses. Groups of 10 eye discs were illuminated for 8 h with red light (~630 nm) at decreasing light pulse frequencies where a 10-s light pulse was provided every 10 s, 1 min, 10 min, or 30 min. β-Actin was used as internal control for normalization. Control samples were kept in dark for the entire duration of the experiment. All data are represented as mean ± S.D.

See also Figures S1, S2, and S5.

PhotoGal4 Drives Light-Dependent Transcription *Ex Vivo*

To demonstrate the light-dependent activity of PhotoGal4 in *ex vivo* cultures, we first crossed GMR-PhotoGal4 flies with flies carrying a UAS-CD8-GFP reporter. Then, from the progeny, we dissected and cultured four sets of 10 eye-antennal discs from third-instar larvae, and incubated them in four different conditions: light, darkness, and absence or presence of the chromophore PCB (100 μM) (Figure 3). The experiment was performed in a closed incubator with a 225 LED lamp placed 3 inches from the top of the *ex vivo* chambers. Fifteen hours after dissection, we observed highly significant GFP expression in samples exposed to continuous red-light pulses (630 nm, 10 s ON/10 s OFF, 0.75mW cm^{-2}) and PCB (Figure 3A, column 4). In contrast, tissues grown in the dark with or without PCB as well as tissues grown under a red light but in the absence of PCB do not have detectable accumulation of GFP protein (Figure 3A, columns 1–3). Next, we tested the ability of PhotoGal4 to activate gene expression in a later stage of development. Thus, we dissected and cultured prepupal retinas throughout 15 h in similar conditions to those described earlier. As expected, prepupal retinas cultured in PCB-supplemented media and exposed to continuous red-light pulses (630 nm, 10 s ON/10 s OFF) showed significantly higher expression of GFP compared with controls ($p < 0.01$) (Figures 3B, 3C, and S2). Overall, these results support the robust PCB- and light-dependent activation of PhotoGal4 in the developing fly eye.

Next, to further determine the versatility of PhotoGal4, we performed experiments at different periods of light irradiation (Figure 3D), under increasing light intensities (Figure 3E), or with different frequencies of light pulses (Figure 3F). For this, we used a customized programmable light-emitting diode (LED) lamp placed half an inch over the plate containing the eye disc explants. To analyze the effect of the duration of stimuli over time, we incubated groups of 10 eye-antennal discs under continuous pulses of light for periods ranging from 0 to 480 min. We opted for long illumination pulses (10 s ON/10 s OFF, 1.2 mW cm^{-2}) to maximize light-induced expression levels (Muller et al., 2014). In our experimental conditions, global red-light irradiation is innocuous to cells when working in ranges of intensities between 0 and 2 mW cm^{-2} and cycles equal or inferior to 10 s. Thus, 8 h after the initial light pulse, we harvested all samples and processed them for mRNA. As anticipated, CD8-GFP mRNA levels correlated with the duration of light exposure showing a 2-fold expression level only after 2 h, reaching ~100-fold after 8 h (Figure 3D). In contrast, control groups expressing PhotoGal4 in the presence of PCB but without light failed to activate the CD8-GFP reporter transgene. Then, to assess the effect of light potency, we tested four different intensities including I50, I30, I15, and I1, correlating with ~100% (1.9 mW cm^{-2}), ~60% (1.2 mW cm^{-2}), ~30% (0.6 mW cm^{-2}), and ~2% (0.05 mW cm^{-2}) of maximum LED intensity, respectively. We found that high GFP expression levels correlate directly with high light intensity values (Figure 3E). Last, we performed experiments at different frequencies of light/dark pulses including 10 s/10 s, 10 s/1 min, 10 s/10 min, and 10 s/30 min (630 nm 1.2 mW cm^{-2}). All groups were cultured under the same conditions of light intensity and PCB concentration (100 μM) for 8 h before harvesting. As expected, GFP protein levels decreased as the light pulses became sparser in time (Figure 3F). Altogether, these data demonstrate that PhotoGal4 can regulate gene expression levels in a customized manner by simply adjusting conditions of the light stimuli such as intensity, duration of exposure, or frequency of light cycles.

PhotoGal4 Activity Is Fully Reversible

One of the most interesting and unique features of the PhyB-based optogenetic system is its capability to be switched off under far-red irradiation (>720 nm). To test whether the light-dependent activity of PhotoGal4 could be reversed, we exposed *ex vivo* cultures of developing eye discs to pulses of 10 s of 630 nm light (1.2 mW cm^{-2}) and 10 s of >750 nm (1.9 mW cm^{-2}) filtered bright-field light followed by 1 min of darkness. As far-red pulses are provided immediately after red pulses, the PhyB/Pif6 interaction induced by red light is expected to dissociate immediately after far-red light exposure. Accordingly, tissues exposed to far-red light showed a significant decrease in GFP accumulation compared with those tissues exposed exclusively to red light (Figures 4A and 4B), suggesting that PhotoGal4 was effectively inactivated. Quantification of GFP mRNA confirmed the significant differences between activated and inactivated

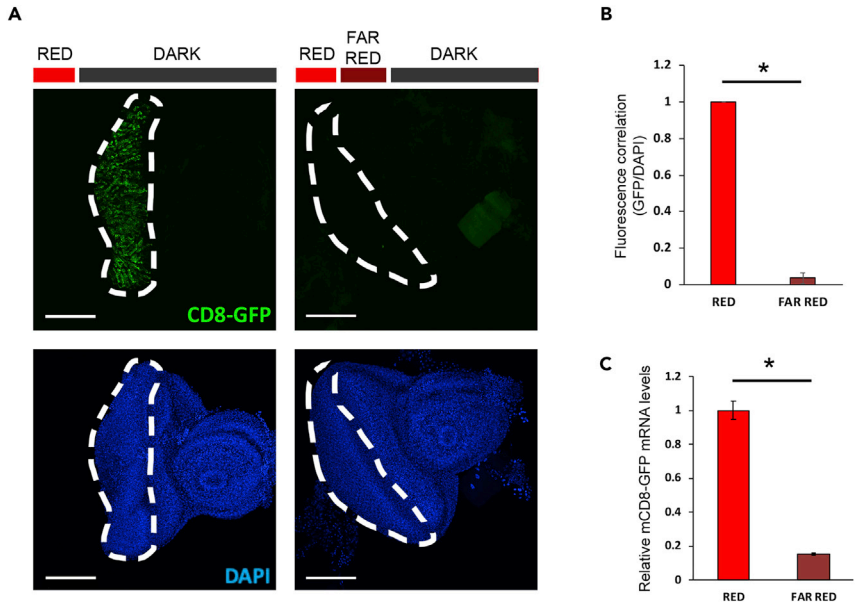

Figure 4. Far-Red Light Reverses PhotoGal4 Function

(A) Reversibility of PhotoGal4-dependent expression of CD8-GFP in eye imaginal discs cultured *ex vivo* with PCB. Samples were subjected to 10-s pulses of red light alone or followed by 10 s of filtered far-red light (>720 nm) and 40 s of darkness for a total period of 8 h. White-dotted lines mark the expected area of PhotoGal4 expression under the GMR promoter. Scale bar, 100 μm.

(B) Fluorescence correlation between samples grown under pulses of red light alone and those exposed to red and far-red light treatments (averaged values of n = 3). *$p < 0.01$ by two-tailed Student's t test. The data are represented as mean ± S.D.

(C) Quantification of GFP mRNA levels from samples treated with red or red and far-red light. Values were normalized to RP49 internal transcripts. *$p < 0.01$ by two-tailed Student's t test. The data are represented as mean ± S.D.

See also Figure S3.

PhotoGal4-expressing tissues ($p < 0.01$) (Figure 4C). Besides, to confirm that PhotoGal4 inactivation was due specifically to far-red irradiation and not to other unforeseen factors, we reproduced the protocol in tissues expressing a mutant version of our system, mutPhotoGal4, whose activation depends solely on PCB administration and functions independently of light (Figures S3A–S3D). Thus, illumination of mutPhotoGal4-expressing tissues with red and/or far-red light should bear no effect on the final levels of gene expression. As predicted, mutPhotoGal4 activation was irreversible after far-red light irradiation and both experimental groups showed similar expression levels of GFP after 8 h of red or red/far-red irradiation (Figure S3E).

PhotoGal4 Allows Optical Sculpting of Gene Expression Patterns

A highly desirable characteristic of any inducible expression system is the ability to easily and selectively activate target genes with fine spatiotemporal resolution. To assess this feature in PhotoGal4, we capitalized on light beams to control the direction of light to specific regions of interest (ROIs). We first demonstrated that a brief irradiation (250 ms every 50 min for 12 h) with the red-light beam (~630 nm, 2.8 mW cm^{-2}) of an inverted widefield microscope at 5 mm distance from the specimen produces comparable GFP fluorescence values to those obtained using LED. Following this protocol, we directed the light beam specifically to one of the two eye discs in a single third-instar larval culture (Figure S4A). As a result, only the eye disc confined within the ROI showed significant levels of GFP expression, whereas its counterpart grown in the dark displayed undetectable levels of GFP (Figure 5A). This suggests that activation of gene expression in particular sub-regions of a tissue carrying PhotoGal4 could be achieved by simply limiting the area of illumination.

To test this hypothesis, we created a more restricted ROI within one single developing eye disc by using a confocal microscope. We first confirmed that exposure to short pulses (150 ms every 50 min for 9 h) of 631-nm laser at low levels (0.5% of maximum laser power) induces similar GFP expression to that obtained with

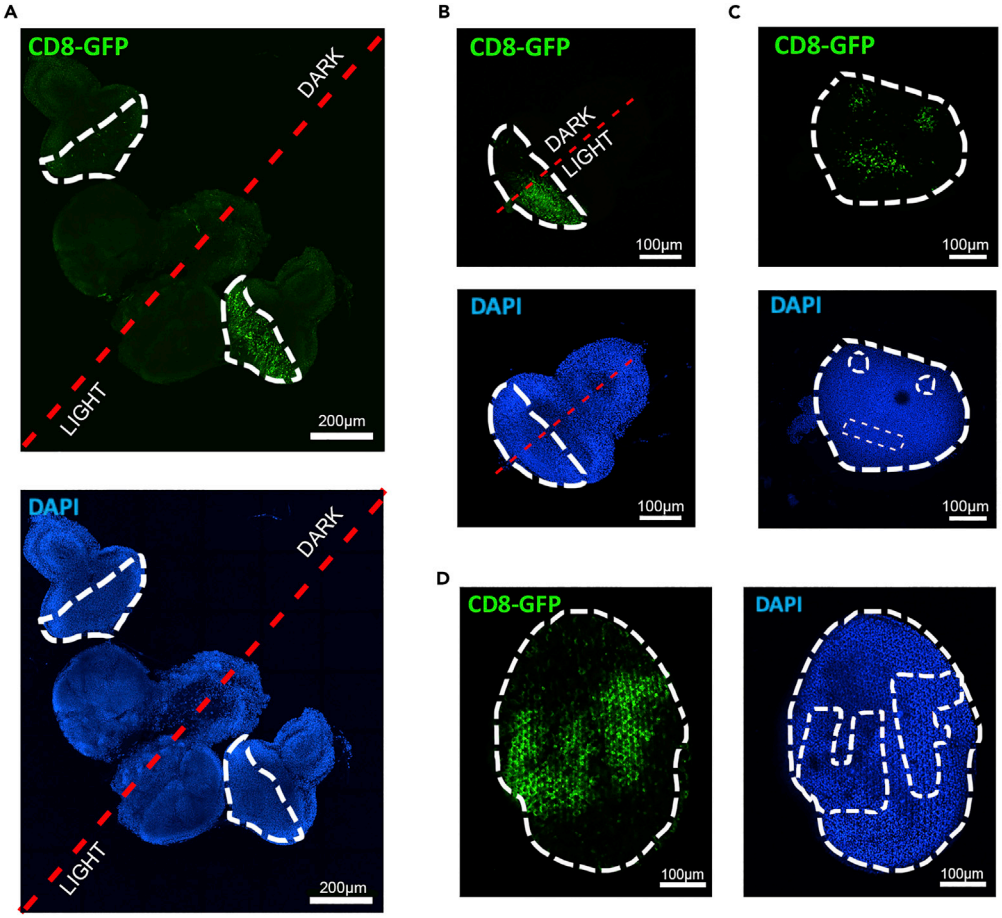

Figure 5. Personalized Activation of PhotoGal4 in the Developing Eye of *Drosophila*

Figure360▷ For a Figure360 author presentation of Figure 5, see https://doi.org/10.1016/j.isci.2020.101308.

(A) Specific activation of CD8-GFP expression in only one of the two eye discs connected to the brain of a single third-instar *Drosophila* larva. A widefield microscope was used to direct 250-ms pulses of 630 nm every 50 min for a total period of 15 h to only one of the two eye discs cultured *ex vivo* with 100 μM PCB. Note that GFP is detected within the expression domain of the GMR promoter (white dotted lines) only in the presence of light. Red dotted lines delimit the areas kept in darkness or exposed to red light. Scale bar, 200 μm.

(B) Regions of interest were created to activate CD8-GFP expression in only one-half of the GMR territory (white dotted lines) within the eye imaginal disc. Specimens were exposed to 150-ms pulses of 561 nm at 0.5% laser power from a confocal fluorescent microscope every 30 min for 8 h and cultured for a total period of 15h (7 h in dark). Scale bar, 100 μm.

(C) Manipulation of PhotoGal4 to imprint a happy face-like pattern of GFP expression within the pupal retina. Scale bar, 100 μm.

(D) A PhotoGal4-induced "GFP tattoo" showing the initials of the University of Florida (UF) in the pupal retina. Scale bar, 100 μm. All final images are projections of z stack captures for DAPI (351 nm) and GFP (488 nm) channels.

See also Figures S4 and S5.

the LED light source. Then, we manipulated the laser beam to specifically illuminate only one-half of the GMR territory while keeping the other half in the dark (Figure S4B). Although all the eye primordium express PhotoGal4 through the GMR promoter (Figure S1), only the half exposed to the red-light beam displayed GFP accumulation within the ROI (Figure 4B). Next, we decided to go one step further and explored the possibility of generating more complex patterns of expression. Given that prepupal retinas offer a bigger canvas to operate, we used this paradigm to imprint "GFP tattoos" in distinct configurations within the GMR territory. Thus, we designed ROIs to specifically engrave an "emoji-like" face as well as the initials of the University of Florida (UF). Strikingly, we successfully engraved the expected "GFP tattoos" upon red-light illumination (Figures 5C and 5D). These extraordinary results indicate that even intricate sub-patterns of gene expression can be created within the same tissue (Figure 5D), highlighting the versatility and specificity of the PhotoGal4 system.

DISCUSSION

Despite the tremendous contribution of classic *Drosophila* gene expression systems, there is still a need for more time-restrictive and spatial-accurate tools to improve our understanding of many biological processes. The emergence of a new generation of tools based on light-sensitive proteins aimed to fill this gap (de Mena et al., 2018). As light acts as the stimuli, these optogenetic systems promised a faster and finer way of selectively activating gene expression with minimal side effects. Thus, motivated by this technology, we implemented PhotoGal4, a multipurpose PhyB-based optogenetic switch, to regulate gene expression in *Drosophila* tissues.

Over the years, different photo-sensing proteins have been adapted to manipulate gene expression. For instance, within the blue-light spectrum, systems such as EL222 or CRY-CIB effectively trigger gene expression in different animal cell models (Motta-Mena et al., 2014; Pathak et al., 2013; Reade et al., 2017; Taslimi et al., 2016). However, these systems require constant light stimulation for activation because removal of the stimuli results in deactivation (de Mena et al., 2018). In contrast, PhyB-based systems are uniquely attractive because they can be turned ON and OFF by switching between red or far-red light for an unlimited period of time. Moreover, activated PhyB remains stable during its half-life, allowing for shorter periods of red-light pulses at longer intervals, which reduces the risk of phototoxicity compared with blue-light systems (Buckley et al., 2016; de Mena et al., 2018; Levskaya et al., 2009; Pathak et al., 2013). Unfortunately, no PhyB-based optogenetic system is yet available for manipulation of gene expression in *Drosophila*.

The first attempt to bring optogenetics to the *Drosophila* community for transgene control proposed a blue-light expression system. The authors created a UAS cassette carrying the light-responsive CRY2/CIBN heterodimer components hooked to the split LexA transcriptional activator (Chan et al., 2015). In this concept, a fully functional LexA is reconstituted upon activation through any Gal4 driver and blue-light illumination, resulting in expression of a target gene fused to the LexAop promoter. This platform worked well in *Drosophila* cultured cells and showed up to 10-fold activation of a GFP reporter; however, it displayed elevated basal transcription levels *in vivo* even in dark conditions. As a solution, the authors introduced a feedback mechanism through the transcriptional repressor Gal80, which reduces the strength of the Gal4-dependent UAS-CRY2/CIBN-LexA construct, but at the same time complicates genetic manipulation. Besides, this system relies on the LexAop promoter for gene activation, whose application is limited compared with thousands of available UAS strains. To bypass these limitations, we opted for a PhyB-based system that could be exploited to manipulate expression of any available UAS transgene with high versatility and low background.

When tested in *Drosophila* cultured cells, PhotoGal4 consistently induced more than 20-fold increase in reporter gene expression under standard light conditions with negligible background (Figures 2B–2D). We then capitalized on the relatively flat structure of the eye imaginal disc to fully assess the transcriptional attributes of PhotoGal4 in *Drosophila* tissues *ex vivo* (Figures S5A and S5B). We demonstrated that PhotoGal4 allows for a high level of spatiotemporal regulation (Figures 3A and 3B) with low background (Figures 3D–3F) and rapid photo-reversibility (Figure 4). Of note, we found that the system facilitates fine-tune regulation of gene induction through modification of the red-light conditions. For instance, a higher frequency and duration of red-light pulses correlated with an increment in the expression levels of the reporter gene (Figures 3D and 3F). A boost in the intensity of the light source also led to higher expression levels (Figure 3E). Besides, we observed that reporter gene expression was already perceptible by qRT-PCR within 2 h after PhotoGal4 activation (Figure 3D). These results suggest that manipulation of the red-light conditions such as duration of stimuli, number of cycles, and intensity of light could potentially allow for user-defined levels of final transcriptional products.

On the other hand, the bicistronic nature of PhotoGal4 provides simplicity and flexibility, making it easier to operate in *Drosophila* (Figures 2A and S1A). For instance, the engineering of PhotoGal4 allows for easy exchange of tissue-specific driver sequences, facilitating its use in a broad range of tissues and organs. However, the most interesting feature of PhotoGal4 is its unique ability to switch it off. Most optogenetic transcriptional regulators rely on the spontaneous return to the dark state of the photo-sensing protein to cease gene expression (Di Ventura and Kuhlman, 2016; Pathak et al., 2014), whereas far-red light permits switching off PhyB-based tools almost instantly at any desirable moment (Buckley et al., 2016; de Mena et al., 2018; Levskaya et al., 2009; Pathak et al., 2013). Our results demonstrated that providing pulses of far-red light immediately after activating red light pulses reversed PhotoGal4 to its inactive form, resulting

in a lack of reporter gene expression (Figure 4). We believe that this reversibility will be instrumental to selectively switch ON/OFF gene expression at will at different experimental points and/or developmental stages.

Unlike classical chemically inducible systems, the use of targeted light to activate PhotoGal4 allows sculpting of complex spatial patterns in a particular group of cells. Here, we demonstrated that PhotoGal4 has the ability to restrict gene expression to a specific organ (Figure 5A), defined areas within that organ (Figure 5B), and even sophisticated patterns of expression in different shapes (Figures 5C and 5D). This is achieved by simply creating ROIs with a confocal microscope. However, in theory, specialized microscopy involving digital micromirror device or two-photon technology could provide more restricted patterns of expression, potentially even to a single-cell resolution.

In conclusion, this work demonstrates that PhotoGal4 can be used as a high-resolution device to sculpt gene expression in response to light quantity, duration of exposure, and trajectory of the beam. We anticipate that the ability to control gene expression "a la carte" will provide *Drosophila* researchers with customizable platforms to study gene function at specific times and sites, with switching options, and possibly in a dose-dependent manner. Thus, further implementation of PhotoGal4 in intact flies may play a transformative role in promoting widespread applications of optogenetics to achieve ultrasensitive and reversible manipulation of any gene in *Drosophila* with remarkable precision.

Limitations of the Study

Some limitations of our study must be acknowledged. Our system requires exogenous chromophore (PCB) for proper PhotoGal4 function. However, we believe that the addition of PCB exogenously acts as an extra safeguard for fly manipulation and experimentation. Most photo-sensing inducible systems require working under safelight conditions and total avoidance of environmental white light to remain inactive (Hernandez-Candia et al., 2019). In contrast, the PCB-dependent function of PhotoGal4 permits safe handling of specimens under standard light conditions until PCB is incorporated, reducing the risk of undesired photo-activation and leakiness. Another potential issue is that the supplemented PCB may not reach proper concentrations in certain tissues *in vivo*, which may affect the potency of PhotoGal4. However, it has been shown that mammalian cultured cells expressing cyanobacterial enzymes PcyA and HO1 can successfully transform endogenous heme groups into PCB (Kyriakakis et al., 2018; Muller et al., 2013b; Uda et al., 2017; Youichi Uda et al., 2020). We strongly believe that genetic synthesis of PCB will pave the way for more practical applications of PhotoGal4.

Another potential drawback is that PhyB-based systems can be activated by wavelengths below the 630-nm spectrum under certain conditions. In our hands, long exposures of high intensity blue or green light led to significant expression of reporter gene (data not shown), coinciding with previous reports (Adrian et al., 2017). However, this could be bypassed by immediately providing cycles of deactivating far-red light pulses. In this regard, when far-red light irradiates the tissue, PhyB becomes inactive and dissociates from Pif6, which precludes further target gene activation. It is worth to mention, however, that all previously activated proteins will remain in the cell for the duration of their half-life. This should be taken into consideration when performing gene expression experiments that require narrow periods of activation and deactivation.

Last, PhotoGal4 functions specifically in *ex vivo* paradigms at present. Therefore, one final concern refers to its future implementation in adult intact flies due to cuticle and tissue penetration issues. Previous studies indicate that red and far-red light systems provide higher penetration than those associated with blue and UV wavelengths, while showing less phototoxicity (Ash et al., 2017; Kwon et al., 2009). However, accurate targeting of deep tissues within live organisms remains a challenge due to dispersion and diffusion of light through multiple cell layers. Fortunately, this scenario is changing with the development of new live imaging approaches. For instance, surgical windows in head and thorax of living fruit flies are becoming common practice for central nervous system imaging in freely walking flies (Chen et al., 2018; Huang et al., 2018; Simpson and Looger, 2018). Similarly, adaptation of multiphoton microscopy to live flies is facilitating high-definition imaging of deep structures such as the brain mushroom bodies (Aragon et al., 2019). Thus, we believe that the combination of these technologies with PhotoGal4 will capture the imagination of the community and stimulate exciting new ideas to expand the horizons and applications of our system in the future.

Resource Availability

Lead Contact

Requests for resources and reagents should be directed to and will be fulfilled by the Lead Contact, Diego E. Rincon-Limas (diego.rincon@neurology.ufl.edu).

Materials Availability

All constructs and *Drosophila* lines generated in this study will be made available on request to the Lead Contact without restriction; however, requestor will cover shipping costs. This study did not generate new unique reagents.

Data and Code Availability

Requests for raw data can be directed to the Lead Contact. All the DNA sequences for constructs designed in this study are located within Transparent Methods. This study did not generate large datasets, computer codes, or algorithms.

METHODS

All methods can be found in the accompanying Transparent Methods supplemental file.

SUPPLEMENTAL INFORMATION

Supplemental Information can be found online at https://doi.org/10.1016/j.isci.2020.101308.

ACKNOWLEDGMENTS

We thank Dr. Jared Toettcher for providing the blueprints and software to create and manipulate the RED LED programmable lamp. We also thank all Rincon-Limas lab members for valuable discussions. This work was supported by NIH grants R21NS088866 and R01AG059871 to D.E.R.-L., by an HHMI-sponsored post-doctoral fellowship from the Life Sciences Research Foundation to L.D.M, and by NIH Grant 1S10OD020026 to the University of Florida CTAC core for the Nikon A1RMP system.

AUTHOR CONTRIBUTIONS

L.D.M. and D.E.R.-L designed the study; L.D.M. performed the experiments; L.D.M. and D.E.R.-L. analyzed data; L.D.M. and D.E.R.-L. wrote and edited the manuscript.

DECLARATION OF INTERESTS

The authors declare no competing interests.

Received: March 29, 2020
Revised: May 15, 2020
Accepted: June 19, 2020
Published: July 24, 2020

REFERENCES

Adrian, M., Nijenhuis, W., Hoogstraaten, R.I., Willems, J., and Kapitein, L.C. (2017). A phytochrome-derived photoswitch for intracellular transport. ACS Synth. Biol. *6*, 1248–1256.

Aragon, M.J., Wang, M., Shea, J., Mok, A.T., Kim, H., Lett, K.M., Barkdull, N., Schaffer, C.B., Xu, C., and Yapici, N. (2019). Non-invasive multiphoton imaging of neural structure and activity in Drosophila. bioRxiv. https://doi.org/10.1101/798686.

Ash, C., Dubec, M., Donne, K., and Bashford, T. (2017). Effect of wavelength and beam width on penetration in light-tissue interaction using computational methods. Lasers Med. Sci. *32*, 1909–1918.

Auldridge, M.E., and Forest, K.T. (2011). Bacterial phytochromes: more than meets the light. Crit. Rev. Biochem. Mol. Biol. *46*, 67–88.

Beyer, H.M., Naumann, S., Weber, W., and Radziwill, G. (2015). Optogenetic control of signaling in mammalian cells. Biotechnol. J. *10*, 273–283.

Buckley, C.E., Moore, R.E., Reade, A., Goldberg, A.R., Weiner, O.D., and Clarke, J.D. (2016). Reversible optogenetic control of subcellular protein localization in a live vertebrate embryo. Dev. Cell *36*, 117–126.

Chan, Y.B., Alekseyenko, O.V., and Kravitz, E.A. (2015). Optogenetic control of gene expression in Drosophila. PLoS One *10*, e0138181.

Chen, C.L., Hermans, L., Viswanathan, M.C., Fortun, D., Aymanns, F., Unser, M., Cammarato, A., Dickinson, M.H., and Ramdya, P. (2018). Imaging neural activity in the ventral nerve cord of behaving adult Drosophila. Nat. Commun. *9*, 4390.

Davis, S.J., Vener, A.V., and Vierstra, R.D. (1999). Bacteriophytochromes: phytochrome-like photoreceptors from nonphotosynthetic eubacteria. Science *286*, 2517–2520.

de Mena, L., Rizk, P., and Rincon-Limas, D.E. (2018). Bringing light to transcription: the optogenetics repertoire. Front. Genet. *9*, 518.

Di Ventura, B., and Kuhlman, B. (2016). Go in! Go out! Inducible control of nuclear localization. Curr. Opin. Chem. Biol. *34*, 62–71.

Fischer, J.A., Giniger, E., Maniatis, T., and Ptashne, M. (1988). GAL4 activates transcription in Drosophila. Nature *332*, 853–856.

Hay, B.A., Wolff, T., and Rubin, G.M. (1994). Expression of baculovirus P35 prevents cell death in Drosophila. Development *120*, 2121–2129.

Hernandez-Candia, C.N., Wysoczynski, C.L., and Tucker, C.L. (2019). Advances in optogenetic regulation of gene expression in mammalian cells using cryptochrome 2 (CRY2). Methods *164-165*, 81–90.

Huang, C., Maxey, J.R., Sinha, S., Savall, J., Gong, Y., and Schnitzer, M.J. (2018). Long-term optical brain imaging in live adult fruit flies. Nat. Commun. *9*, 872.

Hughes, R.M., Bolger, S., Tapadia, H., and Tucker, C.L. (2012). Light-mediated control of DNA transcription in yeast. Methods *58*, 385–391.

Kwon, K., Son, T., Lee, K.J., and Jung, B. (2009). Enhancement of light propagation depth in skin: cross-validation of mathematical modeling methods. Lasers Med. Sci. *24*, 605–615.

Kyriakakis, P., Catanho, M., Hoffner, N., Thavarajah, W., Hu, V.J., Chao, S.S., Hsu, A., Pham, V., Naghavian, L., Dozier, L.E., et al. (2018). Biosynthesis of orthogonal molecules using ferredoxin and ferredoxin-NADP(+) reductase systems enables genetically encoded PhyB optogenetics. ACS Synth. Biol. *7*, 706–717.

Landis, G.N., Salomon, M.P., Keroles, D., Brookes, N., Sekimura, T., and Tower, J. (2015). The progesterone antagonist mifepristone/RU486 blocks the negative effect on life span caused by mating in female Drosophila. Aging (Albany NY) *7*, 53–69.

Levskaya, A., Weiner, O.D., Lim, W.A., and Voigt, C.A. (2009). Spatiotemporal control of cell signalling using a light-switchable protein interaction. Nature *461*, 997–1001.

Mezan, S., Feuz, J.D., Deplancke, B., and Kadener, S. (2016). PDF signaling is an integral part of the drosophila circadian molecular oscillator. Cell Rep. *17*, 708–719.

Motta-Mena, L.B., Reade, A., Mallory, M.J., Glantz, S., Weiner, O.D., Lynch, K.W., and Gardner, K.H. (2014). An optogenetic gene expression system with rapid activation and deactivation kinetics. Nat. Chem. Biol. *10*, 196–202.

Muller, K., Engesser, R., Metzger, S., Schulz, S., Kampf, M.M., Busacker, M., Steinberg, T., Tomakidi, P., Ehrbar, M., Nagy, F., et al. (2013a). A red/far-red light-responsive bi-stable toggle switch to control gene expression in mammalian cells. Nucleic Acids Res. *41*, e77.

Muller, K., Engesser, R., Timmer, J., Nagy, F., Zurbriggen, M.D., and Weber, W. (2013b). Synthesis of phycocyanobilin in mammalian cells. Chem. Commun. (Camb) *49*, 8970–8972.

Muller, K., Engesser, R., Timmer, J., Zurbriggen, M.D., and Weber, W. (2014). Orthogonal optogenetic triple-gene control in Mammalian cells. ACS Synth. Biol. *3*, 796–801.

Osterwalder, T., Yoon, K.S., White, B.H., and Keshishian, H. (2001). A conditional tissue-specific transgene expression system using inducible GAL4. Proc. Natl. Acad. Sci. U S A *98*, 12596–12601.

Pathak, G.P., Strickland, D., Vrana, J.D., and Tucker, C.L. (2014). Benchmarking of optical dimerizer systems. ACS Synth. Biol. *3*, 832–838.

Pathak, G.P., Vrana, J.D., and Tucker, C.L. (2013). Optogenetic control of cell function using engineered photoreceptors. Biol. Cell *105*, 59–72.

Prithviraj, R., Trunova, S., and Giniger, E. (2012). Ex vivo culturing of whole, developing Drosophila brains. J. Vis. Exp. 4270, https://doi.org/10.3791/4270.

Reade, A., Motta-Mena, L.B., Gardner, K.H., Stainier, D.Y., Weiner, O.D., and Woo, S. (2017). TAEL: a zebrafish-optimized optogenetic gene expression system with fine spatial and temporal control. Development *144*, 345–355.

Shimizu-Sato, S., Huq, E., Tepperman, J.M., and Quail, P.H. (2002). A light-switchable gene promoter system. Nat. Biotechnol. *20*, 1041–1044.

Simpson, J.H., and Looger, L.L. (2018). Functional imaging and optogenetics in Drosophila. Genetics *208*, 1291–1309.

Stramer, B., and Wood, W. (2009). Inflammation and wound healing in Drosophila. Methods Mol. Biol. *571*, 137–149.

Sun, Y., Chen, X., and Xiao, D. (2007). Tetracycline-inducible expression systems: new strategies and practices in the transgenic mouse modeling. Acta Biochim. Biophys. Sin (Shanghai) *39*, 235–246.

Tanguay, R.M. (1988). Transcriptional activation of heat-shock genes in eukaryotes. Biochem. Cell Biol. *66*, 584–593.

Taslimi, A., Zoltowski, B., Miranda, J.G., Pathak, G.P., Hughes, R.M., and Tucker, C.L. (2016). Optimized second-generation CRY2-CIB dimerizers and photoactivatable Cre recombinase. Nat. Chem. Biol. *12*, 425–430.

Tsao, C.K., Ku, H.Y., Lee, Y.M., Huang, Y.F., and Sun, Y.H. (2016). Long term ex vivo culture and live imaging of Drosophila larval imaginal discs. PLoS One *11*, e0163744.

Tsao, C.K., Ku, H.Y., and Sun, Y.H. (2017). Long-term live imaging of Drosophila eye disc. J. Vis. Exp. 55748, https://doi.org/10.3791/55748.

Uda, Y., Goto, Y., Oda, S., Kohchi, T., Matsuda, M., and Aoki, K. (2017). Efficient synthesis of phycocyanobilin in mammalian cells for optogenetic control of cell signaling. Proc. Natl. Acad. Sci. U S A *114*, 11962–11967.

Youichi Uda, H.M., Goto, Yuhei, and Aoki, Kazuhiro (2020). Improvement of phycocyanobilin synthesis for genetically encoded phytochrome-based optogenetics. bioRxiv. https://doi.org/10.1101/2020.1101.1115.908343.

iScience, Volume *23*

Supplemental Information

PhotoGal4: A Versatile Light-Dependent Switch for Spatiotemporal Control of Gene Expression in *Drosophila* Explants

Lorena de Mena and Diego E. Rincon-Limas

Supplemental Figures

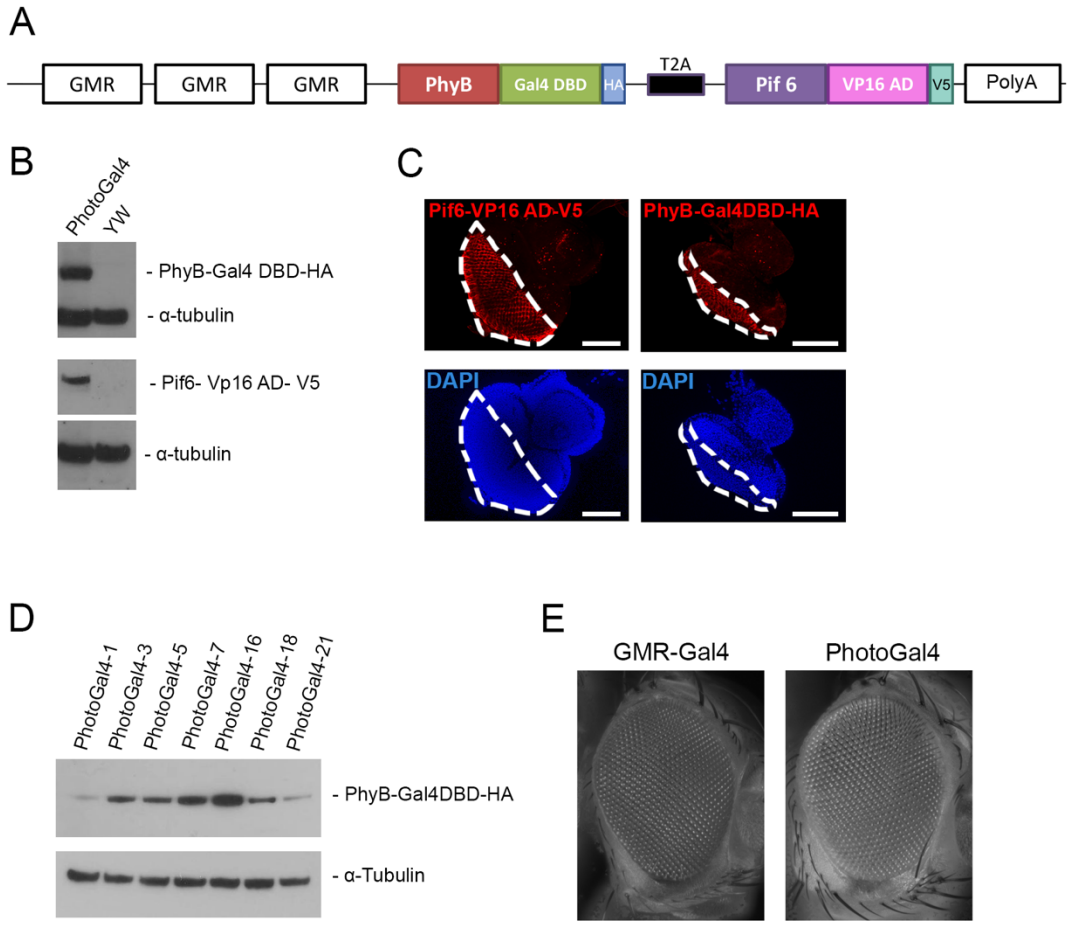

Figure S1. PhotoGal4 expression in the developing eye of *Drosophila*. (Related to Figure 3)
(A) Schematic representation of the PhotoGal4 construct used in all *Drosophil*a ex vivo experiments. Three copies of the GMR promoter regulate PhotoGal4, which consists of a PhyB 650aa sequence fused to Gal4 DBD and the HA tag, and Pif 6 fused to the transcriptional activation domain of VP16 and the V5 tag, separated by the T2A sequence.
(B) Western blot analysis of protein lysates from transgenic flies expressing PhotoGal4 components. Protein lysates from *yw* flies were used as a negative control to assess specific immunoreactivity against HA and V5 tags, and α-tubulin was used as the internal control.
(C) Immunodetection of Pif6-VP16AD-V5 and PhyB-Gal4DBD-HA in third instar larval eye imaginal discs with anti-V5 (left) and Anti-HA (right) antibodies. Dotted area marks the GMR expression domain. The scale bar is 100 µm.
(D) A total of seven homozygous lines were obtained for GMR-PhotoGal4. Line 16 showed the highest expression level and was used throughout the paper.
(E) Fresh eye pictures from control flies (GMR-Gal4, left) or flies expressing PhotoGal4 line 16 (right). No apparent toxicity was appreciated.

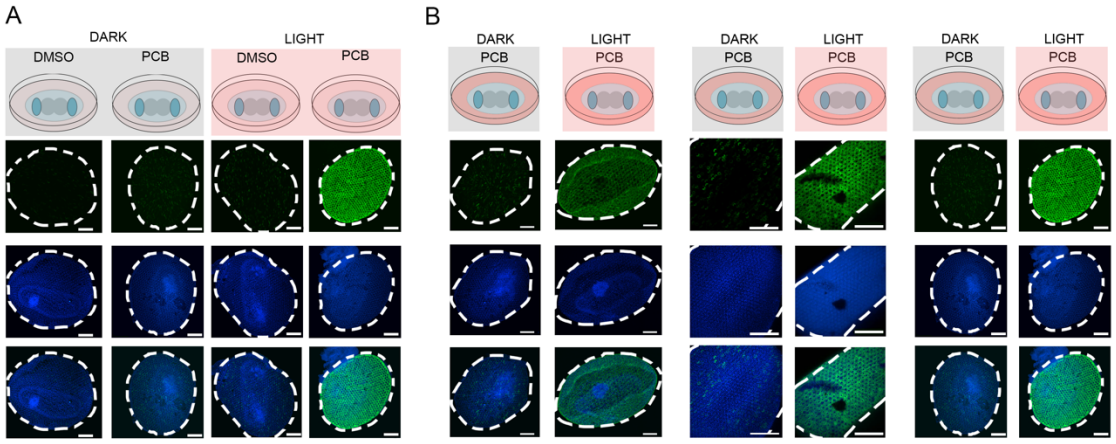

Figure S2. PhotoGal4 activates gene expression in the *Drosophila* prepupal retina in a light-dependent manner. (Related to Figures 3B and 3C)

(A) Prepupal retinas from flies expressing PhotoGal4 and UAS-mCD8-GFP constructs were dissected and grown in ex vivo culture media supplemented with 100μM PCB or DMSO, either in the dark or under constant pulses of red light for 15h (10s on 10s off) (n=6 for each condition). The scale bar is 100 μm.

(B) Group of prepupal retinas (n=3) used for the relative fluorescent correlation shown in Figure 3C. Each image is the result of a projection of a z-stack capture. White-dotted lines mark the area where the GMR promoter drives PhotoGal4 expression. The scale bar is 100 μm.

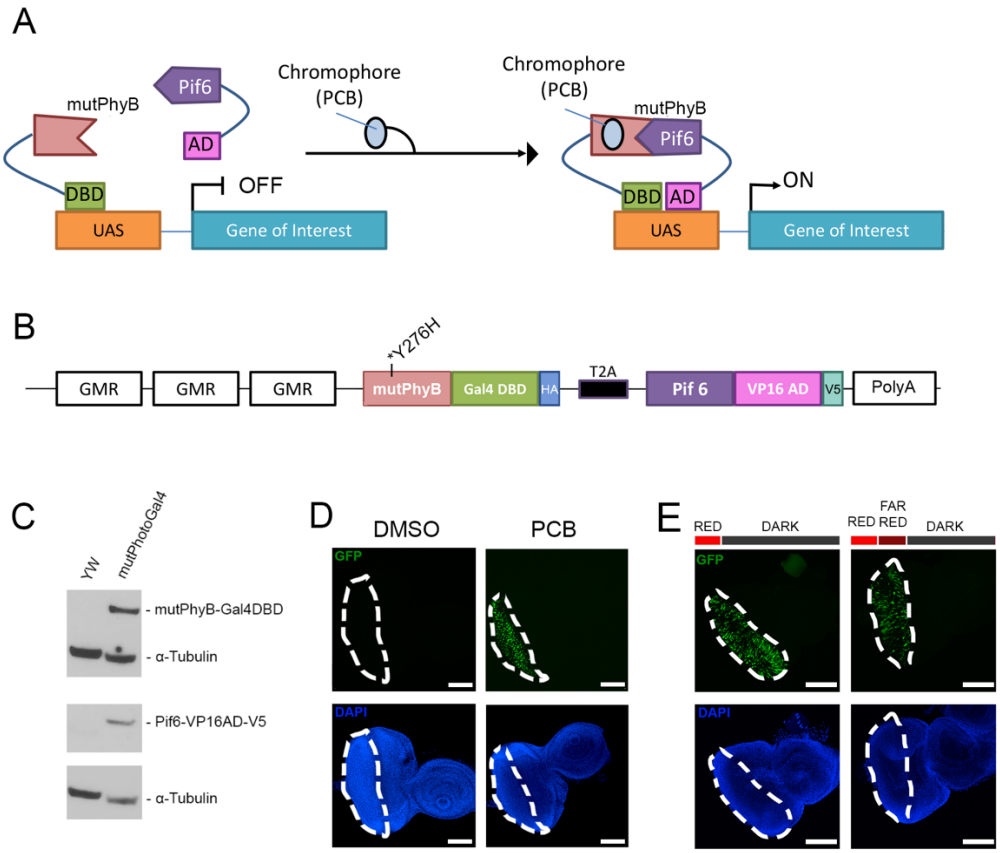

Figure S3. PCB-dependent activation of mutPhotoGal4 in the developing eye of *Drosophila*. (Related to Figure 4)

(A) Schematic representation of the mutPhotoGal4 PCB-dependent gene expression system. In absence of chromophore PCB, mutant phytochrome B (mutPhyB) remains in its inactive form. Upon incorporation of PCB to the medium, mutPhyB-Gal4DBD gets activated and heterodimerizes with Phytochrome-interacting factor Pif6 to bring together Gal4DBD and VP16AD, triggering gene transcription.

(B) Structural organization of the mutPhotoGal4 construct. The mutPhotoGal4 system consists of the PhyB 650aa sequence harboring mutation Y276H fused to Gal4 DBD and the HA tag, and Pif6 fused to the transcriptional activation domain of VP16 and the V5 tag. Both chimeric proteins are separated by a T2A sequence and regulated by the three copies of the GMR promoter.

(C) Western blot analysis of mutPhotoGal4 components in the developing eye of third instar larvae. Protein lysates from *yw* larvae were used as a negative control and α-tubulin was used as internal control.

(D) PCB-dependent activation of mutPhotoGal4. Eye imaginal discs expressing mutPhotoGal4 and UAS-GFP constructs were dissected and grown in ex vivo culture media supplemented with 100uM PCB or DMSO (n=6 for each condition). White-dotted lines mark the area where the GMR promoter drives mutPhotoGal4 expression and scale bar is 100um.

(E) Far-red light does not inhibit mutPhotoGal4 activity. Eye imaginal discs carrying mutPhotoGal4 and UAS-CD8-GFP constructs were cultured in ex vivo medium containing 100uM of PCB. Samples were subjected to 10s pulses of red light alone or either followed by 10s of filtered far-red light (>720nm) and then by 40s of darkness for a total period of 8h (n=6 for each condition). Each image is the result of a projection of a z-stack capture. White-dotted lines mark the area where the GMR promoter drives mutPhotoGal4 expression. The scale bar is 100um.

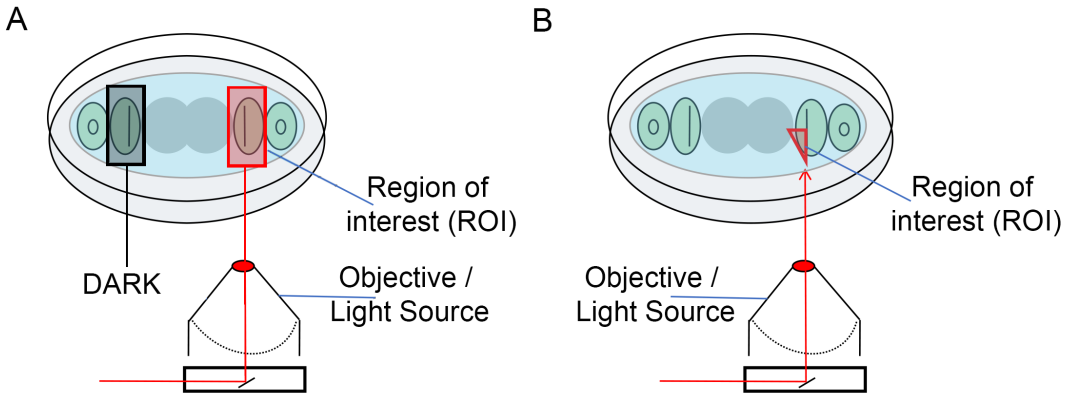

Figure S4. Experimental settings for the spatial activation of PhotoGal4 in the developing *Drosophila* eye. (Related to Figure 5)
(A) This example shows how the light beam of a widefield microscope is directed to only one of the two eye discs attached to the third instar larval brain in an ex vivo chamber (pink rectangle).
(B) In this case, the beam of a confocal fluorescent microscope is directed toward a specific region of interest (ROI) comprising a small group of cells within a single eye disc (red triangle).

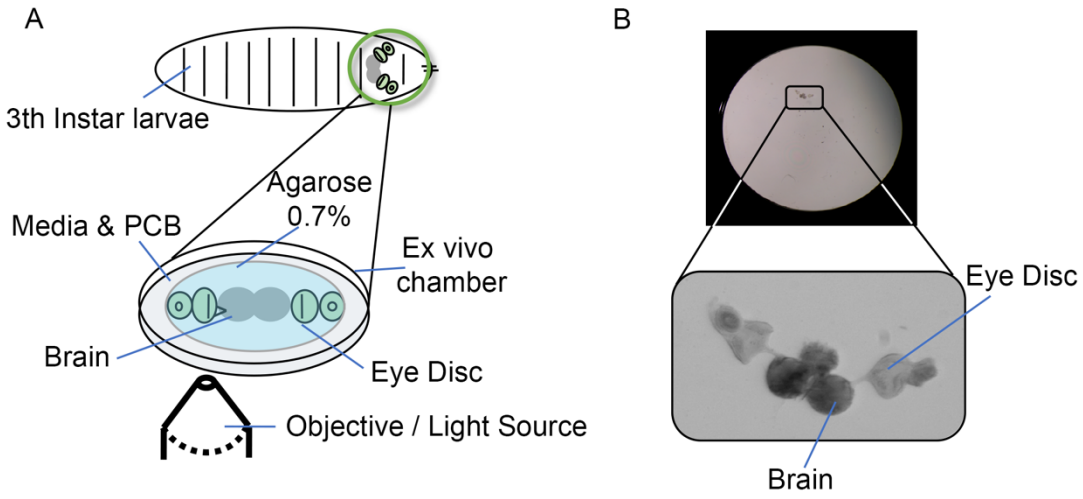

Figure S5. Visual representation of ex vivo culture chambers. (Related to Figures 3, 4 and 5)
(A) *Drosophila* third instar larval eye discs are dissected bound to the brain, mounted in a glass-bottom dish, and covered with 0.7% gel of low-melting agarose and PBS 1x. After gelification, tissues are covered with 1ml of ex vivo culture media supplemented with PCB.
(B) Brightfield image of a real ex vivo chamber and eye disc-brain-eye disc complex used in this manuscript.

Transparent Methods

***Drosophila* S2R+ cell culture and transfection**

Drosophila embryonic SR2+ cells (DGRC stock number #150) were cultured in the dark in Schneider medium at 25°C supplemented with 10% bovine serum albumin (FBS, Thermofisher) and 1% penicillin/streptomycin. To assess the expression and distribution of PhotoGal4 components, 4 x 10^5 cells were co-transfected in duplicate with 200 ng of actin-PhotoGal4 and UAS-CD8-GFP vectors in 24-well plates using the Qiagen Effectene Kit (#301425, Qiagen) and supplemented with 10µM PCB when needed. Then, 24 h after transfection, cell cultures were kept either in dark or exposed to LED red light cycles (630 nm, 2501BU, LED Wholesalers) for another 24 h. The LED cycles consisted of pulses of 10s on and 1min off controlled by an electronic timer (Model 451, GraLab). Transfected cells were collected and processed for western blot analysis, immunostaining or dual-luciferase assay as described below. Luciferase activities were measured using the Dual-luciferase reporter assay kit (#E1910, Promega) following the manufacturer's instructions.

Generation of PhotoGal4 constructs

The PhotoGal4 expression cassette was engineered to contain the PhyB 1-650 aa fragment fused to Gal4-DBD and the HA tag followed by a T2A skipping ribosomal sequence, and then the chimeric gene Pif6 (1-100 aa) fused to the VP16 AD and the V5 tag. This cassette was synthesized and cloned into the pUC57 vector (GenScript), which facilitates the release of PhotoGal4 with restriction enzymes for further subcloning (see sequences below).

For PhotoGal4 expression in S2R+ cell cultures, we subcloned the PhotoGal4 cassette into a pAC5 empty vector via Not1/Kpn1 sites to generate the light-dependent pActin-PhotoGal4 construct.

To target the expression of PhotoGal4 in the developing eye of the fly, we first created a *Drosophila* expression vector carrying three copies of the GMR promoter sequence. For this, we replaced the five copies of UAS sequences in the plasmid pUAST with a customized sequence containing three copies of the GMR promoter sequence (5'-CCCAGTGGAAACCCTTGAAATGCCTTTAAGTCGAG-3') fused to the Hsp70 mini-promoter via PstI/EcoRI ligation, which generated the vector pGMR-linker. Sequences corresponding to the GMR promoter, TATA box and polylinker are as follows:

*CCCAGTGGAAACCCTTGAAATGCCTTTAAGTCGAG*CCCAGTGGAAACCCTTGAAATGCCTTT
AAGTCGAG*CCCAGTGGAAACCCTTGAAATGCCTTTAAGTCGAG*GTCGAC**ACGCGT**GGCGAA
AAGAGCGCCGGAGTATAAATAGAGGCGCTTCGTCTACGGAGCGACAATTCAATTCAAACAA
GCAAAGTGAACACGTCGCTAAGCGAAAGCTAAGCAAATAAACAAGCGCAGCTGAACAAGCT
AAACAATCTCCAGTAAAGTGCAAGTTAAAGTGAATCAATTAAAAGTAACCAGCAACCAAGTAA
ATCAACTGCAACTACTGAAATCTGCCAAGAAGTAATTATTGAATACAAGAAGAGAACTCTGAA
TAGG**AGATCTGAATTCGCGGCCGCGGTACCTCTAGA**

Underline italics: GMR sequences (3x)
Bold: restriction enzyme
Yellow and bold: Polylinker
Blue highlight: Hsp70TATA-box

Then, to create pGMR-PhotoGal4, we simply inserted the PhotoGal4 cassette into pGMR-linker via NotI and KpnI sites. The sequence of the GMR-PhotoGal4 expression cassette is the following:

*CCCAGTGGAAACCCTTGAAATGCCTTTAAGTCGAG*CCCAGTGGAAACCCTTGAAATGCCTTT
AAGTCGAG*CCCAGTGGAAACCCTTGAAATGCCTTTAAGTCGAG*GTCGAC**ACGCGT**GGCGAA
AAGAGCGCCGGAGTATAAATAGAGGCGCTTCGTCTACGGAGCGACAATTCAATTCAAACAA
GCAAAGTGAACACGTCGCTAAGCGAAAGCTAAGCAAATAAACAAGCGCAGCTGAACAAGCT

AAACAATCTCCAGTAAAGTGCAAGTTAAAGTGAATCAATTAAAAGTAACCAGCAACCAAGTAA
ATCAACTGCAACTACTGAAATCTGCCAAGAAGTAATTATTGAATACAAGAAGAGAACTCTGAA
TAGG**AGATCTGAATTCGCGGCCGC**ACACCATGGTGAGCGGCGTGGGCGGCAGCGGCGGC
GGACGCGGCGGCGGACGCGGCGGCGAGGAGGAGCCCAGCAGCAGCCACACCCCCAACAA
CCGCCGCGGCGGCGAGCAGGCCCAGAGCAGCGGCACCAAGAGCCTGCGCCCCCGCAGCA
ACACCGAGAGCATGAGCAAGGCCATCCAGCAGTACACCGTGGATGCCCGCCTGCACGCCG
TGTTCGAGCAGAGCGGCGAGAGCGGCAAGAGCTTCGATTACAGCCAGAGCCTGAAGACCA
CCACCTACGGCAGCAGCGTGCCCGAGCAGCAGATCACCGCCTACCTGAGCCGCATCCAGC
GCGGCGGCTACATCCAGCCCTTCGGCTGCATGATCGCCGTGGATGAGAGCAGCTTCCGCA
TCATCGGCTACAGCGAGAACGCCCGCGAGATGCTGGGCATCATGCCCCAGAGCGTGCCCA
CCCTGGAGAAGCCCGAGATCCTGGCCATGGGCACCGATGTGCGCAGCCTGTTCACCAGCA
GCAGCAGCATCCTGCTGGAGCGCGCCTTCGTGGCCCGCGAGATCACCCTGCTGAACCCCG
TGTGGATCCACAGCAAGAACACCGGCAAGCCCTTCTACGCCATCCTGCACCGCATCGATGT
GGGCGTGGTGATCGATCTGGAGCCCGCCCGCACCGAGGATCCCGCCCTGAGCATCGCCG
GCGCCGTGCAGAGCCAGAAGCTGGCCGTGCGCGCCATCAGCCAGCTGCAGGCCCTGCCC
GGCGGCGATATCAAGCTGCTGTGCGATACCGTGGTGGAGAGCGTGCGCGATCTGACCGGC
TACGATCGCGTGATGGTGTACAAGTTCCACGAGGATGAGCACGGCGAGGTGGTGGCCGAG
AGCAAGCGCGATGATCTGGAGCCCTACATCGGCCTGCACTACCCCGCCACCGATATCCCCC
AGGCCAGCCGCTTCCTGTTCAAGCAGAACCGCGTGCGCATGATCGTGGATTGCAACGCCAC
CCCCGTGCTGGTGGTGCAGGATGATCGCCTGACCCAGAGCATGTGCCTGGTGGGCAGCAC
CCTGCGCGCCCCCCACGGCTGCCACAGCCAGTACATGGCCAACATGGGCAGCATCGCCAG
CCTGGCCATGGCCGTGATCATCAACGGCAACGAGGATGATGGCAGCAACGTGGCCAGCGG
ACGCAGCAGCATGCGCCTGTGGGGCCTGGTGGTGTGCCACCACACCAGCAGCCGCTGCAT
CCCCTTCCCCCTGCGCTACGCCTGCGAGTTCCTGATGCAGGCCTTCGGCCTGCAGCTGAAC
ATGGAGCTGCAGCTGGCCCTGCAGATGAGCGAGAAGCGCGTGCTGCGCACCCAGACCCTG
CTGTGCGATATGCTGCTGCGCGATAGCCCCGCCGGCATCGTGACCCAGAGCCCCAGCATC
ATGGATCTGGTGAAGTGCGATGGCGCCGCCTTCCTGTACCACGGCAAGTACTACCCCCTGG
GCGTGGCCCCCAGCGAGGTGCAGATCAAGGATGTGGTGGAGTGGCTGCTGGCCAACCACG
CCGATAGCACCGGCCTGAGCACCGATAGCCTGGGCGATGCCGGCTACCCCGGCGCCGCC
GCCCTGGGCGATGCCGTGTGCGGCATGGCCGTGGCCTACATCACCAAGCGCGATTTCCTG
TTCTGGTTCCGCAGCCACACCGCCAAGGAGATCAAGTGGGGCGGCGCCAAGCACCACCCC
GAGGATAAGGATGATGGCCAGCGCATGCACCCCCGCAGCAGCTTCCAGGCCTTCCTGGAG
GTGGTGAAGAGCCGCAGCCAGCCCTGGGAGACCGCCGAGATGGATGCCATCCACAGCCTG
CAGCTGATCCTGCGCGATAGCTTCAAGGAGAGCGAGGCCGCCATGAACAGCAAGGTGGTG
GATGGCGTGGTGCAGCCCTGCCGCGATATGGCCGGCGAGCAGGGCATCGATGAGCTGGG
CG**ATTTAAATACGCGT***GATAGTGCCGGAAGTGCCGGAAGTGCCGGAACG***CGTAGATCT***AT**
GAAGCTGCTGTCCAGTATTGAGCAGGCCTGCGACATTTGCCGCCTGAAGAAGCTGAAGTGC
AGCAAGGAGAAGCCCAAGTGCGCCAAGTGCCTGAAGAACAATTGGGAGTGCCGCTACAGTC
CGAAGACCAAGCGCAGCCCACTGACACGCGCCCACCTGACCGAGGTGGAGTCGCGCCTGG
AGCGCCTGGAGCAGCTGTTCCTGCTGATCTTTCCCCGCGAGGATCTGGACATGATTCTGAA
GATGGATTCGCTGCAGGACATCAAGGCCCTGCTGACAGGCCTGTTCGTGCAGGATAACGTG
AATAAGGATGCCGTGACCGATCGCCTGGCCTCCGTGGAGACCGACATGCCGCTGACACTG
CGCCAGCACCGCATTAGTGCCACCAGCTCCTCGGAGGAGAGTAGCAACAAGGGCCAGCGC
***CAGCTGACCGTGTCC*ACTAGT*TACCCCTATGATGTGCCCGACTACGCC*GCTAGC*GAGGGAC**
GCGGATCGCTGCTGACCTGCGGCGATGTGGAGGAGAACCCAGGACCC**CTCGAG**ATGATGT
TCCTGCCAACGGATTACTGCTGCCGCCTGAGCGACCAGGAGTATATGGAGCTGGTGTTTGA
GAATGGCCAGATTCTGGCCAAGGGACAGCGCAGTAACGTGAGCCTGCACAATCAGCGCAC
CAAGTCGATCATGGATCTGTACGAGGCCGAGTATAACGAGGACTTCATGAAGAGCATCATTC
ATGGCGGAGGCGGAGCCATTACCAATCTGGGCGATACGCAGGTGGTGCCCCAGTCCCACG
TGGCCGCCGCCCATGAGACGAACATGCTGGAGTCCAATAAGCACGTGGAC**GGATCC***GCCC*
CACCCACAGATGTGAGTCTGGGCGACGAGCTGCACCTGGATGGAGAGGACGTGGCCATGG
CCCATGCCGATGCCCTGGATGACTTCGATCTGGATATGCTGGGCGATGGAGACAGCCCCG
GACCAGGATTTACACCACATGACTCGGCCCCATACGGAGCCCTGGATATGGCCGACTTCGA
***GTTTGAGCAGATGTTTACGGATGCCCTGGGAATCGACGAGTATGGCGGC*TCTAGAACCGGT**
***GGCAAGCCGATTCCGAACCCGCTGCTGGGACTGGACTCGACG*ACCGGTTGA**GGTACCTCT
AGA

Underline italics: GMR sequences (3x)
Bold: restriction enzymes
Yellow highlight: Hsp70 TATA-box
Yellow and bold: Polylinker
Pink highlight: Kozac sequence
Green highlight: PhyB (650aa)
Pink highlight and bold: flexible protein linker
Green highlight and italics: Gal4-DBD and HA tag
Red Highlight: T2A ribosomal skipping sequence
Grey highlight: Pif6 (100aa)
Grey highlight and italics: VP16-AD and V5 tag
Bold and underline italics: Stop codon

To create the pGMR-mutPhotoGal4 vector, we introduced the Y276H mutation by site directed mutagenesis with primers mutPhyBY276H-Fw (5'-CCTCGTGGAACTTGTGCACCATCACGC GATC-3') and mutPhyBY276H-Rv (5'-GATCGCGTGATGGTGCACAAGTTCCACGAGG-3') using the Phusion site-directed mutagenesis kit (#F541, ThermoFisher Scientific). The sequence of the pGMR-mutPhotoGal4 is as follows:

*CCCAGTGGAAACCCTTGAAATGCCTTTAAGTCGAG*CCCAGTGGAAACCCTTGAAATGCCTTT
*AAGTCGAGCCCAGTGGAAACCCTTGAAATGCCTTTAAGTCGAG*GTCGAC**ACGCGT**GGCGAA
AAGAGCGCCGGAGTATAAATAGAGGCGCTTCGTCTACGGAGCGACAATTCAATTCAAACAA
GCAAAGTGAACACGTCGCTAAGCGAAAGCTAAGCAAATAAACAAGCGCAGCTGAACAAGCT
AAACAATCTCCAGTAAAGTGCAAGTTAAAGTGAATCAATTAAAAGTAACCAGCAACCAAGTAA
ATCAACTGCAACTACTGAAATCTGCCAAGAAGTAATTATTGAATACAAGAAGAGAACTCTGAA
TAGG**AGATCTGAATTCGCGGCCGC**ACACCATGGTGAGCGGCGTGGGCGGCAGCGGCGGC
GGACGCGGCGGCGGACGCGGCGGCGAGGAGGAGCCCAGCAGCAGCCACACCCCCAACAA
CCGCCGCGGCGGCGAGCAGGCCCAGAGCAGCGGCACCAAGAGCCTGCGCCCCCGCAGCA
ACACCGAGAGCATGAGCAAGGCCATCCAGCAGTACACCGTGGATGCCCGCCTGCACGCCG
TGTTCGAGCAGAGCGGCGAGAGCGGCAAGAGCTTCGATTACAGCCAGAGCCTGAAGACCA
CCACCTACGGCAGCAGCGTGCCCGAGCAGCAGATCACCGCCTACCTGAGCCGCATCCAGC
GCGGCGGCTACATCCAGCCCTTCGGCTGCATGATCGCCGTGGATGAGAGCAGCTTCCGCA
TCATCGGCTACAGCGAGAACGCCCGCGAGATGCTGGGCATCATGCCCCAGAGCGTGCCCA
CCCTGGAGAAGCCCGAGATCCTGGCCATGGGCACCGATGTGCGCAGCCTGTTCACCAGCA
GCAGCAGCATCCTGCTGGAGCGCGCCTTCGTGGCCCGCGAGATCACCCTGCTGAACCCCG
TGTGGATCCACAGCAAGAACACCGGCAAGCCCTTCTACGCCATCCTGCACCGCATCGATGT
GGGCGTGGTGATCGATCTGGAGCCCGCCCGCACCGAGGATCCCGCCCTGAGCATCGCCG
GCGCCGTGCAGAGCCAGAAGCTGGCCGTGCGCGCCATCAGCCAGCTGCAGGCCCTGCCC
GGCGGCGATATCAAGCTGCTGTGCGATACCGTGGTGGAGAGCGTGCGCGATCTGACCGGC
TACGATCGCGTGATGG***TGC***ACAAGTTCCACGAGGATGAGCACGGCGAGGTGGTGGCCGAG
AGCAAGCGCGATGATCTGGAGCCCTACATCGGCCTGCACTACCCCGCCACCGATATCCCCC
AGGCCAGCCGCTTCCTGTTCAAGCAGAACCGCGTGCGCATGATCGTGGATTGCAACGCCAC
CCCCGTGCTGGTGGTGCAGGATGATCGCCTGACCCAGAGCATGTGCCTGGTGGGCAGCAC
CCTGCGCGCCCCCCACGGCTGCCACAGCCAGTACATGGCCAACATGGGCAGCATCGCCAG
CCTGGCCATGGCCGTGATCATCAACGGCAACGAGGATGATGGCAGCAACGTGGCCAGCGG
ACGCAGCAGCATGCGCCTGTGGGGCCTGGTGGTGTGCCACCACACCAGCAGCCGCTGCAT
CCCCTTCCCCCTGCGCTACGCCTGCGAGTTCCTGATGCAGGCCTTCGGCCTGCAGCTGAAC
ATGGAGCTGCAGCTGGCCCTGCAGATGAGCGAGAAGCGCGTGCTGCGCACCCAGACCCTG
CTGTGCGATATGCTGCTGCGCGATAGCCCCGCCGGCATCGTGACCCAGAGCCCCAGCATC
ATGGATCTGGTGAAGTGCGATGGCGCCGCCTTCCTGTACCACGGCAAGTACTACCCCCTGG
GCGTGGCCCCCAGCGAGGTGCAGATCAAGGATGTGGTGGAGTGGCTGCTGGCCAACCACG
CCGATAGCACCGGCCTGAGCACCGATAGCCTGGGCGATGCCGGCTACCCCGGCGCCGCC
GCCCTGGGCGATGCCGTGTGCGGCATGGCCGTGGCCTACATCACCAAGCGCGATTTCCTG
TTCTGGTTCCGCAGCCACACCGCCAAGGAGATCAAGTGGGGCGGCGCCAAGCACCACCCC

GAGGATAAGGATGATGGCCAGCGCATGCACCCCCGCAGCAGCTTCCAGGCCTTCCTGGAG
GTGGTGAAGAGCCGCAGCCAGCCCTGGGAGACCGCCGAGATGGATGCCATCCACAGCCTG
CAGCTGATCCTGCGCGATAGCTTCAAGGAGAGCGAGGCCGCCATGAACAGCAAGGTGGTG
GATGGCGTGGTGCAGCCCTGCCGCGATATGGCCGGCGAGCAGGGCATCGATGAGCTGGG
CG**ATTTAAATACGCGT***GATAGTGCCGGAAGTGCCGGAAGTGCCGGAACG***CGTAGATCT***AT**
GAAGCTGCTGTCCAGTATTGAGCAGGCCTGCGACATTTGCCGCCTGAAGAAGCTGAAGTGC
AGCAAGGAGAAGCCCAAGTGCGCCAAGTGCCTGAAGAACAATTGGGAGTGCCGCTACAGTC
CGAAGACCAAGCGCAGCCCACTGACACGCGCCCACCTGACCGAGGTGGAGTCGCGCCTGG
AGCGCCTGGAGCAGCTGTTCCTGCTGATCTTTCCCCGCGAGGATCTGGACATGATTCTGAA
GATGGATTCGCTGCAGGACATCAAGGCCCTGCTGACAGGCCTGTTCGTGCAGGATAACGTG
AATAAGGATGCCGTGACCGATCGCCTGGCCTCCGTGGAGACCGACATGCCGCTGACACTG
CGCCAGCACCGCATTAGTGCCACCAGCTCCTCGGAGGAGAGTAGCAACAAGGGCCAGCGC
*CAGCTGACCGTGTCC****ACTAGT****TACCCCTATGATGTGCCCGACTACGCC****GCTAGC***GAGGGAC
GCGGATCGCTGCTGACCTGCGGCGATGTGGAGGAGAACCCAGGACCC**CTCGAG**ATGATGT
TCCTGCCAACGGATTACTGCTGCCGCCTGAGCGACCAGGAGTATATGGAGCTGGTGTTTGA
GAATGGCCAGATTCTGGCCAAGGGACAGCGCAGTAACGTGAGCCTGCACAATCAGCGCAC
CAAGTCGATCATGGATCTGTACGAGGCCGAGTATAACGAGGACTTCATGAAGAGCATCATTC
ATGGCGGAGGCGGAGCCATTACCAATCTGGGCGATACGCAGGTGGTGCCCCAGTCCCACG
TGGCCGCCGCCCATGAGACGAACATGCTGGAGTCCAATAAGCACGTGGAC**GGATCC***GCCC*
CACCCACAGATGTGAGTCTGGGCGACGAGCTGCACCTGGATGGAGAGGACGTGGCCATGG
CCCATGCCGATGCCCTGGATGACTTCGATCTGGATATGCTGGGCGATGGAGACAGCCCCG
GACCAGGATTTACACCACATGACTCGGCCCCATACGGAGCCCTGGATATGGCCGACTTCGA
*GTTTGAGCAGATGTTTACGGATGCCCTGGGAATCGACGAGTATGGCGGC***TCTAGAACCGGT**
*GGCAAGCCGATTCCGAACCCGCTGCTGGGACTGGACTCGACG****ACCGGTTGA***GGTACCTCT**
AGA

Underline italics: GMR sequences (3x)
Bold: restriction enzymes
Yellow highlight: Hsp70 TATA-box
Yellow and bold: Polylinker
Pink highlight: Kozac sequence
Green highlight: PhyB (650aa)
Pink highlight and bold: flexible protein linker
Green highlight and italics: Gal4-DBD and HA tag
Green highlight and bold italics: codon inducing Y276H mutation
Red Highlight: T2A ribosomal skipping sequence
Grey highlight: Pif6 (100aa)
Grey highlight and italics: VP16-AD and V5 tag
Bold and underline italics: Stop codon

All sequences listed above were codon optimized for *Drosophila melanogaster* and sequenced in both strands upon subcloning to confirm the identity and integrity of the sequence.

Drosophila stocks and generation of transgenic flies

All fly stocks and crosses used for light induction experiments were kept at 25°C under regular lab conditions of light and Fisherbrand Jazz-Mix *Drosophila* food. The UAS-mCD8-GFP fly stock was obtained from the Bloomington *Drosophila* Stock Center. Flies expressing GMR-PhotoGal4 and GMR-mutPhotoGal4 constructs were generated by P-element-mediated transformation into *yw* embryos (Rainbow Transgenics, Inc). Seven homozygous viable lines were created with GMR-PhotoGal4, two of them in chromosome 3 (lines 1 and 21) and four in chromosome 2 (lines 3, 5, 7, and 16). One homozygous line was obtained for mutPhotoGal4. The line with the highest expression level of PhotoGal4 components was chosen for this work (PhotoGal4-16) (Figure S1D). Homozygous expression of this line was innocuous in the structure and morphology of the adult eye (Figure S1E).

Larval and pupal ex vivo cultures

All utensils used for dissections (forceps, needles and 9-well glass dissection plates) were soaked in 70% ethanol for 20 min and allowed to dry for 10 min. Larvae were selected at the third instar stage, rinsed in water, soaked in 70% ethanol (<5min) and dissected in approximately 300 µl of 1% phosphate-buffered saline (PBS). Dissected tissues were subsequently placed in ex-vivo culture media for posterior light treatments and qPCR and WB analysis. Alternatively, dissected eye discs were mounted in a glass-bottom dish and embedded in 0.7% gel of low-melting agarose (#0815-25G, VWR Ameresco life Science) and PBS 1x (#10010-023, Gibco by Life Technologies) for spatiotemporal light treatments. Samples were incubated for 2 min to ensure gelification and then covered with 1 ml of ex-vivo culture medium, which was prepared following Tsao et al. (2016) protocol (Figures S5A and S5B). Briefly, this medium contains Schneider's media (#S0146, Sigma), 2% fetal bovine serum (FBS), 0.5% penicillin/streptomycin (P/S), 10% fly extract (#1645671, DGRC), and 12.5% insulin (#I9278, Sigma). In addition, culture medium was supplemented with the appropriate concentrations of chromophore PCB (#P2172, Sigma Aldrich) when required.

Immunofluorescence

Third instar larval imaginal eye discs or prepupal retinas expressing GMR-PhotoGal4 and UAS-CD8-GFP transgenes were collected and dissected at room temperature under dim white light. Tissues were fixed and stained using mouse anti-HA (1:200, #18181 Abcam) for PhyB-Gal4 DBD-HA and rabbit anti-V5 (1:200, #V8137 Sigma-Aldrich) for Pif6-VP16 AD-V5. Secondary antibody anti-mouse-Cy3 (#A10522, ThermoFisher Scientific) was used at 1:600 and tissues were mounted in Vectashield antifade mounting medium (#H-1000, Vector Laboratories). Six fields per coverslip were captured and analyzed for protein expression and distribution.

Western blot analysis

S2R cells or ex vivo culture tissues were respectively homogenized in 100ul or 30ul of RIPA buffer (#89900, ThermoFisher Scientific) supplemented with 20X proteinase inhibitor (#36978, ThermoFisher Scientific) at 4°C following the manufacturer protocol. Then, equal volumes of protein lysates were independently mixed with NuPage LDS sample buffer (#2083421, Thermo Fisher Scientific) and boiled at 95°C for 5min. Protein extracts were separated by electrophoresis on an SDS-PAGE 4-12% Bis-Tris base gel (NuPage) and transferred to nitrocellulose membranes. Membranes were blocked in 5% non-fat milk and immunostained against the following antibodies: mouse anti-HA (1:200, #18181 Abcam), rabbit anti-V5 (1:200, #V8137 Sigma-Aldrich), mouse anti-GFP (1:2,000; G6795 Sigma Aldrich), α-tubulin (1:500,000; #ab6046 Abcam), or β-actin (1:500; #ab8227, Abcam). Immunoreactive bands were detected by chemiluminescence (#34580 SuperSignal West Pico Plus Chemiluminescent Substrate, Thermo Scientific). Quantification of relative protein expression was performed in three independent experiments and subsequently averaged. ANOVA analysis was used to assess statistical differences between samples using the online open-access tool Quickcalcs GraphPad (GraphPad Prism).

Quantitative RT-PCR (qPCR) analysis

Total RNA was extracted from transfected S2R+ cells and ex vivo tissues using the RNeasy kit (Zymo Research) and subjected to reverse transcription using Superscript III first-strand synthesis kit (#18080051, ThermoFisher Scientific). Quantitative polymerase chain reaction (qPCR) on reporter gene CD8-GFP (CD8-Fw: 5'-TTCTGTCGCTGAACCTGCT-3' and CD8-RV: 5'-AAACGGACCCCAACACTTC-3') and internal control RP49 (RP49-Fw: 5'-AGCACTTCATCCGCCACC-3' and RP49-Rv: 5'- ATCTCGCCGCAGTAAACG-3') were performed using TaqMan Fast Advanced Master Mix with 20 ng of cDNA as template and the CRX96 PCR System (Bio-Rad). Cycling conditions were set at 95°C for 3 min, and 40 cycles of 95°C 15 s and 60°C for 1 min. Triplicates were run for each sample. The average cycle threshold (CT) was

normalized to the corresponding average of RP49 CT value. The fold change in mCD8-GFP mRNA was calculated using the CT (ΔΔCT) method.

Widefield microscopy and image processing

Fluorescent images were collected with AxioVision (Zeiss) in an Axio-Observer Z1 microscope (Zeiss) using ApoTome (structured light microscopy) with 20x NA: 0.7 (air) and 40x NA: 1.3 (air) objectives. As a safety measure to protect the tissue from environmental light, unexposed areas were physically covered with dark tape. Multi-panel figures were created using Adobe Photoshop. Image processing included adjustments of brightness and contrast for optimal viewing of whole images. Identical settings for excitation and detection were used to compare expression levels between samples. Quantification of fluorescence differences between images was performed with ImageJ free software (https://imagej.nih.gov/ij/).

Light treatments

Experiments performed under LED light consisted of groups of five dissected third instar larvae (a total of 10 eye discs) or six prepupal retinas. All tissues were cultured in ex vivo Schneider media in 24 well plates and exposed to light cycles of 10s ON/10s OFF for periods between 8h and 15h as indicated in each experiment. Three independent light culture chambers were created for three different wavelength treatments (630nm, 561nm or 351nm) using a 225 LED lamp with a working voltage of 110-120 volts and a power of 13.8 watts. Light chambers corresponding to control tissues were immediately covered with aluminum foil after dissection and kept in dark for the duration of the experiment to avoid light exposure.

To interrogate the fine-tunable capabilities of PhotoGal4, a programmable LED lamp was used to regulate intensities and cycle frequencies using a customized JAVA program (kindly provided by Dr. Jared Toettcher, Princeton University). For each experiment, groups of 10 dissected eye discs were incubated in culture media in 96-well dark plates with a glass-bottom (# 164588 Thermofisher Scientific) and exposed to the pertinent light protocol. Then, experimental tissues were processed accordingly for western blot, immunostaining, and quantitative PCR.

To quantify light intensities, we used a standard photodiode power sensor (#S120C Thorlabs) connected to a power and energy meter (#PM100D Thorlabs). The photodiode was placed directly underneath the light source and the meter specifically programmed to detect the appropriate wavelength (450nm, 560nm or 630nm). Each measurement was noted in mW cm^{-2}.

Confocal laser scanning light treatment and microscopy

Regions of interest (ROIs) were created using a Nikon confocal microscope through the NIS elements software (NIKON A1RMP). Each ROI was independently scanned with the 647-nm laser beam (125mw) for 150 msec every 25 min for a period of 8h followed by 7h of incubation in dark to ensure maximum reporter gene expression. After a total of 15h of incubation, tissues were fixed and processed for imaging. Adobe Photoshop was used to create the multi-panel figures and brightness and contrast were adjusted for optimal viewing of images. Identical settings for excitation and detection were used to compare expression levels between dark and light samples. Quantification of fluorescence differences between images was performed with ImageJ free software (https://imagej.nih.gov/ij/).

Statistics

For statistical analysis, a two-tailed Student's t-test or ANOVA (as required by the number of samples and means) was applied to compare means represented as mean values ± s.d. P values < 0.05 were considered statistically significant.

Supplemental References

Tsao, C. K., Ku, H. Y., Lee, Y. M., Huang, Y. F., and Sun, Y. H. (2016). Long Term Ex Vivo Culture and Live Imaging of Drosophila Larval Imaginal Discs. PLoS One *11*, e0163744.